Coexistence of *s*-wave superconductivity and phase separation in the half-filled extended Hubbard model with attractive interactions

E. Linnér,[1] C. Dutreix,[2] S. Biermann,[1,3,4,5] and E. A. Stepanov[1,3]
[1]*CPHT, CNRS, École Polytechnique, Institut Polytechnique de Paris, 91120 Palaiseau, France*
[2]*Univ. Bordeaux, CNRS, LOMA, UMR 5798, F-33400 Talence, France*
[3]*Collège de France, 11 place Marcelin Berthelot, 75005 Paris, France*
[4]*Department of Physics, Division of Mathematical Physics, Lund University, Professorsgatan 1, 22363 Lund, Sweden*
[5]*European Theoretical Spectroscopy Facility, 91128 Palaiseau, France*

(Received 23 February 2023; revised 1 November 2023; accepted 6 November 2023; published 29 November 2023)

Understanding competing instabilities in systems with correlated fermions remains one of the holy grails of modern condensed matter physics. Among the fermionic lattice models used to this effect, the extended Hubbard model occupies a prime place due to the potential relevance of its repulsive and attractive versions for both electronic materials and artificial systems. Using the recently introduced multichannel fluctuating field approach, we address the interplay of fluctuations in the charge density wave, *s*-wave superconducting, and phase separation channels in the attractive extended Hubbard model. Despite the fact that this model has been intensively studied for decades, our approach allows us to identify a phase that has not been analyzed before and which is characterized by the coexistence of collective *s*-wave superconducting and phase separation fluctuations. Our findings resonate with previous observations of interplaying phase separation and superconducting phases in electronic systems, most importantly in high-temperature superconductors.

DOI: 10.1103/PhysRevB.108.205156

I. INTRODUCTION

Materials with strong electronic correlations exhibit sophisticated phase diagrams incorporating a complex selection of collective ordering phenomena. The latter are associated with a variety of interplaying instabilities, e.g., charge, spin, or pairing fluctuations. They may appear either in a mutually exclusive form [1,2] or with a stabilization of additional intermediate phases [2–5], e.g., when different fluctuations coexist [6]. An interplay between collective charge, spin, and pairing fluctuations occurs already in the single-band extended Hubbard model [6–11]. Their competition is determined by two parameters: the local U and nonlocal V interactions between electrons. Thus, the model is a suitable framework for a well-controlled investigation of competing instabilities in correlated electronic systems. The local interaction stabilizes collective spin and pseudospin fluctuations in the repulsive [12–15] and attractive [6,15–17] regimes, respectively. Here, pseudospin fluctuations are associated with η-pairing, combining the charge density and s-wave pairing degrees of freedom [18,19]. The spin and pseudospin fluctuations may compete with charge fluctuations that are driven by the nonlocal interaction [11,20,21]. Attractive nonlocal interaction may further promote p- and d-wave superconductivity [22–24]. Strong charge fluctuations may result in the development of the charge density wave (CDW) and phase separation (PS) phases in the repulsive and attractive V cases, respectively.

Significant insights into the collective electronic behavior in the repulsive U, V regime of the extended Hubbard model exist due to extensive research conducted since the 1970's (see, e.g., Refs. [1–6,11,21,25–48]). In contrast, less attention has been paid to the regime of attractive U, dominated by charge fluctuations and s-wave superconductivity (s-SC) [6,15,16,21,23,24,49–66]. The reason is that by its very nature the Coulomb interaction between electrons is repulsive. Nevertheless, it is known that coupling electrons to external degrees of freedom, e.g., phonons, may lead to an effective electronic system with attractive interactions. Specific examples are doped fullerenes [67] and one-dimensional copper oxide chains [68], $Ba_{1-x}K_xBiO_3$ [69,70], $LaAlO_3/SrTiO_3$ interfaces [71–74], and selected d- and f- transition metals [75,76]. In addition, fermionic systems with attractive local interactions are realizable in cold atom experiments [77].

In this work, we focus on the leading collective fluctuations in the half-filled fermionic extended Hubbard model with an attractive local interaction U. We consider both the repulsive and attractive cases for the nonlocal interaction V between neighboring sites on a square lattice. This allows us to investigate the interplay between the CDW, PS, and s-SC instabilities that appear in the system. To this aim, we employ the multichannel fluctuating field (MCFF) approach [47], based on the recently introduced fluctuating local field method [78–82]. Within this approach, a trial system incorporating the main leading collective fluctuations is constructed based on a variational optimization with respect to a reference system. The construction allows us to treat competing fluctuations without any explicit symmetry breaking. Note, a "phase" will in the current work refer to a broader definition including short-range ordering, i.e., transforming into a true phase within a quasi-two-dimensional system. We find that the emergence of a phase combining CDW and s-SC fluctuations is correctly captured at vanishing nonlocal V, signaling the emergent pseudospin SU(2) symmetry of the model. In addition, we discover a coexistence phase composed of PS and s-SC fluctuations spanning a relatively broad region of the attractive U-V phase diagram. Our results obtained within a simple quantum lattice system call for further investigations of novel collective phenomena due to interplaying fluctuations in realistic materials.

II. MODEL AND METHOD

We consider the single-band extended Hubbard model at half-filling on a square lattice, defined by the Hamiltonian

$$\hat{H} = -t \sum_{\langle i,j\rangle,\sigma} \hat{c}^{\dagger}_{i\sigma}\hat{c}_{j\sigma} + U\sum_i \hat{n}_{i\uparrow}\hat{n}_{i\downarrow} + \frac{V}{2}\sum_{\langle i,j\rangle,\sigma\sigma'} \hat{n}_{i\sigma}\hat{n}_{j\sigma'}, \tag{1}$$

where the $\hat{c}^{(\dagger)}_{i\sigma}$ operators correspond to annihilation (creation) of electrons and $\hat{n}_{i\sigma} = \hat{c}^{\dagger}_{i\sigma}\hat{c}_{i\sigma}$ are the electronic densities, with the subscripts denoting the position i and spin projection $\sigma \in \{\uparrow, \downarrow\}$. The kinetics is modeled by a nearest-neighbor hopping amplitude t, with $t = 1$ setting the energy unit. The interaction is modeled by the on-site U and the nearest-neighbor V interactions. Our calculations are for attractive U, while V may be both repulsive and attractive.

The attractive U regime is dominated by charge and s-wave pairing fluctuations. A natural description combining the two channels is the pseudospin, conveniently written using the Nambu basis: $\hat{\psi}_{\mathbf{k},\nu,\uparrow} = \hat{c}_{\mathbf{k}\nu\uparrow}$, $\hat{\psi}_{\mathbf{k},\nu,\downarrow} = \hat{c}^{\dagger}_{-\mathbf{k}+\mathbf{M},\nu\downarrow}$, $\hat{\psi}^{\dagger}_{\mathbf{k},\nu,\uparrow} = \hat{c}^{\dagger}_{\mathbf{k}\nu\uparrow}$, and $\hat{\psi}^{\dagger}_{\mathbf{k},\nu,\downarrow} = \hat{c}_{-\mathbf{k}+\mathbf{M},\nu\downarrow}$, with $\mathbf{M} \equiv (\pi, \pi)$. The pseudospin density operator is then defined as

$$\hat{n}^{\varsigma}_{\mathbf{Q}} \equiv \frac{1}{\beta N}\sum_{\mathbf{k},\nu,\sigma\sigma'} \hat{\psi}^{\dagger}_{\mathbf{k}+\mathbf{Q},\nu\sigma}\sigma^{\varsigma}_{\sigma\sigma'}\hat{\psi}_{\mathbf{k}\nu\sigma'}, \tag{2}$$

with the inverse temperature β and number of sites N. The subscripts denote the momentum $\mathbf{k}$ and the fermionic Matsubara frequency ν. Here, the mode is specified by the channel $\varsigma \in \{x, y, z\}$, where $\mathbf{Q}$ is the ordering vector and σ^{ς} are the Pauli spin matrices. Hence, $\hat{n}^{\varsigma}_{\mathbf{Q}}$ refers to the s-wave pairing ($\varsigma \in \{x, y\}$) and the charge fluctuations ($\varsigma \in \{z\}$). The Nambu basis allows for a clear exhibition of the emergence of the SU(2) pseudo-spin symmetry at half-filling in the absence of the nonlocal interaction V [18,19]. In fact, the staggered particle-hole symmetry of the Hubbard model ($V = 0$) relates the spin and pseudospin degrees of freedom [18,19]. Within the charge and s-wave pairing channels, our work focuses on the leading instabilities: the CDW, PS, and s-SC orderings. All three orderings are determined by their respective order parameters, given by the expectation value of the (static) operator $\hat{n}^{\varsigma}_{\mathbf{Q}}$. Here, s-SC and CDW are associated with the ordering vector $\mathbf{Q} = \mathbf{M}$, and PS with $\mathbf{Q} \rightarrow \mathbf{\Gamma} \equiv (0, 0)$ (see the Supplemental Material (SM) [83] for details of the implementation). Within certain regions of the attractive V phase diagram p- and d-wave superconducting phases have also been discussed in the literature [22–24]. In this work, we focus, however, on CDW, PS, and s-SC, excluding other superconducting symmetries. We will come back to this point later.

To study the competing instabilities, we employ the multichannel fluctuating field (MCFF) method [47]. The decisive advantage of this numerical method is the ability to account for the leading fluctuations and their interplay exactly. This

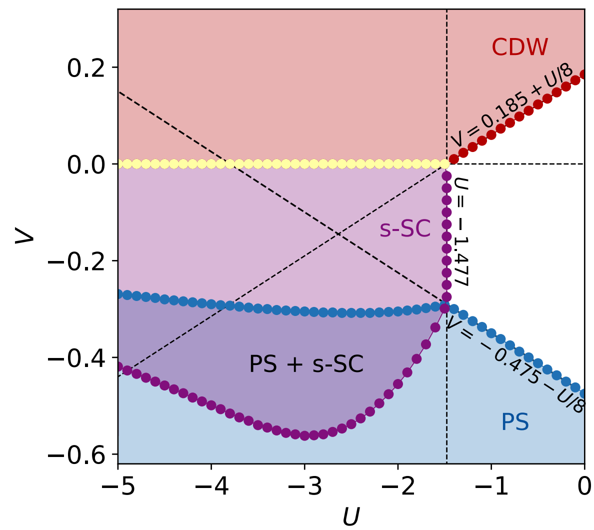

FIG. 1. Phase diagram of the half-filled extended Hubbard model for attractive U. It is obtained from the MCFF method for a 128×128 square lattice with periodic boundary conditions at inverse temperature $\beta = 10$. This shows the existence of a phase "PS + s-SC" where PS and s-SC coexist, in addition to the conventional CDW (red), s-SC (purple), and PS (blue) phases. The yellow line specifies the CDW and s-SC coexistence in the attractive Hubbard model ($V = 0$).

approach is based on the construction of an effective action $\mathcal{S}^*$, where the fluctuations in the charge (CDW, PS) and superconducting channels (s-SC) are incorporated via the associate classical fields $\phi^{\varsigma}_{\mathbf{Q}}$ coupled to the respective components of $\hat{n}^{\varsigma}_{\mathbf{Q}}$ [83]. This construction is determined by the Peierls-Feynman-Bogoliubov variational principle [84–86], with the extended Hubbard model as a reference system. Within the MCFF approach, the interplay between different fluctuations may be determined by a single-channel free energy $\mathcal{F}(\phi^{\varsigma}_{\mathbf{Q}})$. The functional $\mathcal{F}(\phi^{\varsigma}_{\mathbf{Q}})$ is constructed with respect to a classical field $\phi^{\varsigma}_{\mathbf{Q}}$, after integrating out analytically the fermionic degrees of freedom and numerically the remaining classical fields. Phase transitions are then identified by the development of global minima of the single-channel free energy at $\phi^{\varsigma}_{\mathbf{Q}} \neq 0$, akin to a Mexican hat potential. In contrast, a local minimum at $\phi^{\varsigma}_{\mathbf{Q}} \neq 0$ signals metastable collective fluctuations. To obtain further insight into the interplay between collective fluctuations, it is also useful to calculate the corresponding order parameters $\langle\hat{n}^{\varsigma}_{\mathbf{Q}}\rangle$. This can be done by substituting the $\mathcal{F}(\phi^{\varsigma}_{\mathbf{Q}})$ saddle-point value of the classical field $\phi^{\varsigma}_{\mathbf{Q}}$ in the effective action $\mathcal{S}^*$ [83].

III. RESULTS

We perform calculations at $\beta = 10$ for the half-filled extended Hubbard model close to the thermodynamic limit for a square lattice of $N = 128 \times 128$ sites with periodic boundary conditions. Figure 1 shows the resulting U-V phase diagram. It consists of six phases: normal metal (white), CDW (red), s-SC (purple), PS (blue), and two phases where s-SC coexists with either CDW (yellow line) or PS (labeled "PS + s-SC") orderings. At weak coupling ($|U| \lesssim 1.5$), the CDW and PS phase boundaries follow the $V = 0.185 + U/8$ and

$V = -0.475 - U/8$ lines, respectively. These asymptotics are identical to the perturbative estimates for the phase boundaries obtained using the random phase approximation (RPA) in the $U \to 0$ limit. We note that the MCFF approach correctly captures the exact $U \to 0$ limit for the CDW phase boundary, as observed previously in Ref. [47]. In contrast, the PS boundary is slightly overestimated, as an extrapolated $U \to 0$ dual boson result for the PS transition point gives $V^{\rm PS}_{U=0} \simeq -0.54$ [63]. In agreement with the fluctuating exchange (FLEX) result obtained for $V = 0$, the MCFF *s*-SC phase boundary in the weak coupling regime follows the $U^{s-{\rm SC}}_{V=0} = -1.478$ line. FLEX is known to overestimate the strength of antiferromagnetic (AFM) fluctuations at $V = 0$. Therefore, by the staggered particle-hole symmetry of the Hubbard model relating the spin and pseudospin degrees of freedom [18,19], FLEX is also expected to overestimate the strength of the coexisting CDW and *s*-SC fluctuations at $V = 0$. Exploiting this symmetry, in the thermodynamic limit the exact diagrammatic Monte Carlo solution gives $U^{\rm DiagMC}_{V=0} \simeq -2.5$ value at $\beta = 10$ for this transition point [87].

A. Interplay between charge density wave fluctuations and *s*-wave superconductivity

Turning to the intermediate coupling regime, the CDW and *s*-SC fluctuations develop a coexisting phase along the $V = 0$ line displayed in yellow in Fig. 1. This coexistence is associated with the emergent pseudospin symmetry between CDW and *s*-SC order parameters. Beyond this line the finite nonlocal interaction V favors the formation of either the CDW ($V > 0$) or *s*-SC ($V < 0$) phase. Remarkably, we find that at $V \neq 0$ the CDW and *s*-SC phases are mutually exclusive only in the thermodynamic limit. For small-size plaquettes of 4×4, 6×6, and 8×8 lattice sites we find that the CDW and *s*-SC orderings can coexist also in the vicinity of $V = 0$, and the coexistence region decreases with increasing the size of the system [Fig. 2(a)]. This convergence check allows us to identify that the coexistence region in the vicinity of $V = 0$ converges towards a single transition line occurring along $V = 0$ for $U \leqslant -1.447$ in the thermodynamic limit. Thus, the transition between the CDW and *s*-SC phases appearing as a direct first-order phase transition is composed of two first-order phase transitions passing through the intermediate coexistence phase constrained by the pseudo-spin SU(2) symmetry [6].

Another interesting effect can be found in the region of the phase diagram depicted in Fig. 2(b) by green. It displays a region where CDW or *s*-SC orderings are separately stable without interplay between the modes. The dark green area denotes the overlap region of the noncompeting CDW and *s*-SC orderings. In the MCFF method, the CDW phase transition in the presence of the *s*-SC fluctuations is studied by integrating out the *s*-SC modes and investigating the behavior of the free energy $\mathcal{F}(\phi^{\varsigma}_{\mathbf{Q}})$ for the remaining CDW mode, and vice versa. In the region where the integrated *s*-SC mode is ordered, the MCFF analysis of the CDW transition corresponds to the investigation of the stability of the CDW ordering in the presence of the *s*-SC phase. In this regard, the integration of an ordered mode can be seen as an observation or measurement of this ordering in the system. We note that green regions in

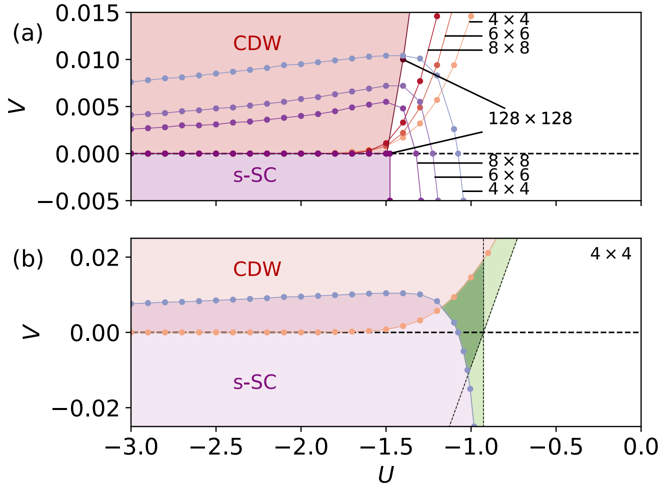

FIG. 2. CDW (red) and *s*-SC (purple) ordering boundaries predicted by the MCFF approach for the half-filled extended Hubbard model obtained for $\beta = 10$: (a) for 4×4, 6×6, 8×8, and 128×128 plaquettes; and (b) for a 4×4 plaquette with the green region enclosed by the thin black dashed lines that depict asymptotics for the noninterplaying CDW and *s*-SC instabilities, displaying the region where the CDW and *s*-SC orderings stabilize without interplay. Dark green denotes the region where stabilization of either the CDW or *s*-SC phase destroys the other ordering.

Fig. 2(b) lie outside the CDW and *s*-SC phases that are obtained considering the interplay between the two fluctuations. Therefore, our results suggest that stabilizing one of the two orderings in the dark green region immediately destroys the other one, which can be seen as a destruction of a quantum superposition of the two orderings by an observer. Remarkably, we find that no such nontrivial "green" phases exist in the thermodynamic limit, where quantum effects are suppressed.

B. Coexistence of *s*-wave superconductivity and phase separation fluctuations

Further, we observe the emergence of a phase that comprises coexisting PS and *s*-SC orderings, sketched in Fig. 3. This PS+*s*-SC phase can be found in the regime of intermediate couplings of the attractive U, V extended Hubbard model (Fig. 1). In contrast to the previously considered coexisting CDW and *s*-SC orderings, this coexistence phase does

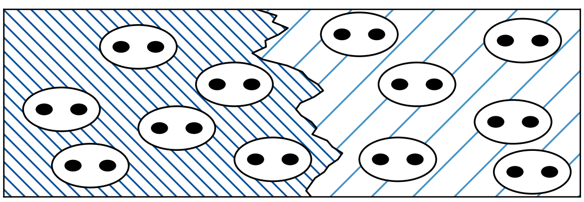

FIG. 3. Cartoon picture of the phase characterized by the coexistence of PS and *s*-SC fluctuations. Within the phase, the collective *s*-SC fluctuations (Cooper pairs depicted by black dots) are sufficiently strong to stabilize the superconducting ordering within the PS puddles with uniform filling larger (left) or smaller (right) than half-filling. The shaded areas represent such regions of higher and lower filling.

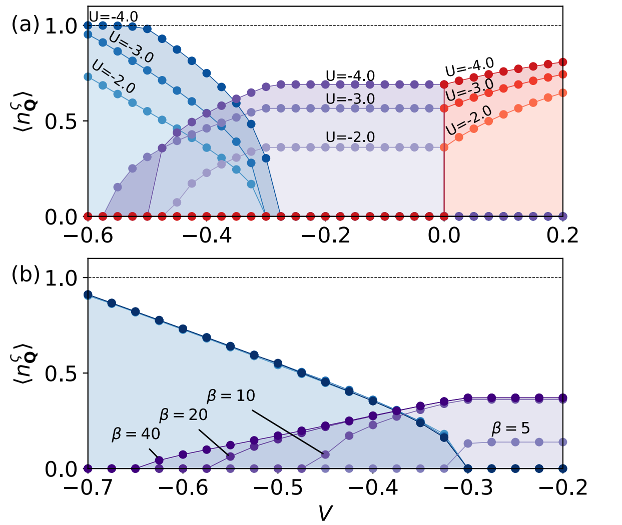

FIG. 4. Normalized order parameters $\langle n^{\varsigma}_{\mathbf{Q}}\rangle$ computed for the half-filled 128 × 128 system using the MCFF approach. (a) CDW (red), *s*-SC (purple), and PS (blue) order parameters are calculated at $\beta = 10$ for $U \in \{-2, -3, -4\}$ for a range of V. (b) *s*-SC (purple) and PS (blue) order parameters calculated at $\beta \in \{5, 10, 20, 40\}$ at $U = -2$ for a range of V.

not collapse to a single transition line in the thermodynamic limit, thus acquiring a finite width in V for a given U. We observe the width to be a nonmonotonic function of U, with a maximal width occurring near $U = -3$. To obtain insight into the interplay between PS and *s*-SC ordering, in Fig. 4(a) we show the normalized CDW, *s*-SC, and PS order parameters $\langle n^{\varsigma}_{\mathbf{Q}}\rangle$ that are computed for $U \in \{-2, -3, -4\}$ over a range of V. We observe a suppression of PS fluctuations in the weak coupling regime $V \gtrsim -0.3$ due to *s*-SC fluctuations, and vice versa at strong V. The competition between these two modes originates from the fact that the PS ordering on a lattice corresponds to the formation of broad puddles with uniform filling larger or smaller than the average filling of the system. Instead, the pairing process of *s*-SC fluctuations is energetically most favorable at half-filling. Due to the stability of the *s*-SC fluctuations for a relatively large range of fillings [50,65], the *s*-SC ordering can be formed inside the PS puddles, which results in the emergence of the coexistence phase. Within the phase, the weights of the PS and *s*-SC modes vary with U, V. Thus, the phase is characterized by the PS and *s*-SC orderings being mutually compatible, i.e., collective *s*-SC fluctuations are stable in the environment of PS ordering and vice versa. As U increases, the region of *s*-SC fluctuations becomes more stable with respect to stronger PS fluctuations, leading to an increasing width of the coexistence region. However, the opposite trend occurs above a critical U as strong PS fluctuations leave the system effectively in an empty or fully-filled sites configuration with $\langle n_{\mathrm{PS}}\rangle = 1$, completely suppressing any *s*-SC fluctuations. Note that the CDW ordering on a square lattice corresponds to a checkerboard pattern of alternating lattice sites with higher and lower electronic densities. This does not allow for the formation of the *s*-SC ordering inside the CDW phase due to the strong inhomogeneity of the filling, except along the degenerate $V = 0$ line due to symmetry constraints.

A recent determinant quantum Monte Carlo (DQMC) study of the zero-temperature U-V phase diagram of the half-filled extended Hubbard model [23] displays a few points of coexisting PS and *s*-SC orderings, evidencing our observations. However, due to the sparsity of the grid in the U-V space, the DQMC results do not allow one to make a statement on the nature of the coexistence phase in the system. In fact, the authors of this work interpret this coexistence as a signature of a first-order transition between the *s*-SC and PS phases. Indeed, first-order transitions are usually accompanied by regions of metastable collective fluctuations appearing as coexistence regions [47]. However, in our work we do not observe metastable collective fluctuations associated with any first-order transition, although the MCFF method allows for their detection in other contexts [47]. This fact allows us to argue for a true coexistence phase stable in the thermodynamic limit enclosed by two apparent second-order transition lines. An order parameter for this phase may be defined as the product of the *s*-SC and PS order parameters. To further connect our finite-temperature calculations to the zero-temperature DQMC results, we compute the *s*-SC and PS order parameters $\langle n^{\varsigma}_{\mathbf{Q}}\rangle$ for $U = -2$ over a range of V at different inverse temperatures $\beta \in \{5, 10, 20, 40\}$. Figure 4(b) shows that the stability of the *s*-SC fluctuations increases with decreasing temperature, as PS fluctuations remain nearly temperature independent. Thus, we expect the phase of coexisting PS and *s*-SC ordering to remain stable at zero temperature and to connect to the results observed in Ref. [23]. The formation of this phase occurs in a region of the U-V phase diagram that is not expected to have contributions from *p*- and *d*-wave superconducting fluctuations [23,24]. This comforts our choice in the present work of not including those fluctuations here.

Exploring the predicted phase diagram experimentally and switching between the different phases in realistic materials could be performed, e.g., by applying an external laser field. In the high-frequency regime of the driving, the applied laser field effectively decreases the hopping amplitude t of electrons [88–94], which effectively enhances the interactions U and V. In the low-frequency regime, driving phonon degrees of freedom may enhance the electron-phonon coupling [95], which would increase the strength of effective attractive electronic interactions [96–98]. This can potentially allow one to propagate within the U-V phase diagram and access the phase characterized by the coexistence of *s*-SC and PS fluctuations.

IV. CONCLUSION

Interplay between SC and PS fluctuations has been observed in high-temperature superconducting materials, such as copper oxides [99–110] and iron-based superconductors [111–116], but the microscopic mechanisms of the observed phenomena remain elusive. In doped copper oxides, it has been argued early on [102,104] that dilute holes in an antiferromagnet have a strong tendency to phase separate. Experimentally, interfaces of $La_{2-x}Sr_xCuO_4$-La_2CuO_4 [109] display an intriguing insensitivity of the critical temperature of the SC phase over an extended range of doping. These findings have been rationalized by invoking interlayer phase separation [110]. Our findings of coexisting SC and PS at half-filling give yet another indication hinting at the possibly very fundamental role of phase separation in the physics of superconducting correlated fermionic systems.

ACKNOWLEDGMENTS

The authors thank M. Chatzieleftheriou for useful discussions and A. Rubtsov for inspiration. E.L., S.B., and E.A.S. acknowledge the help of the CPHT computer support team and the support from IDRIS/GENCI Orsay under Project No. A0130901393. The work of E.L. was supported by funding from the doctoral school of Institut Polytechnique de Paris. C.D. acknowledges the support from Quantum Matter Bordeaux and the SMR department under the projects TED and CDS-QM.

[1] B. Fourcade and G. Spronken, Real-space scaling methods applied to the one-dimensional extended Hubbard model. I. The real-space renormalization-group method, Phys. Rev. B **29**, 5089 (1984).

[2] J. E. Hirsch, Charge-density-wave to spin-density-wave transition in the extended Hubbard model, Phys. Rev. Lett. **53**, 2327 (1984).

[3] M. Nakamura, Mechanism of CDW-SDW transition in one dimension, J. Phys. Soc. Jpn. **68**, 3123 (1999).

[4] M. Nakamura, Tricritical behavior in the extended Hubbard chains, Phys. Rev. B **61**, 16377 (2000).

[5] A. W. Sandvik, L. Balents, and D. K. Campbell, Ground state phases of the half-filled one-dimensional extended Hubbard model, Phys. Rev. Lett. **92**, 236401 (2004).

[6] V. J. Emery, Theory of the quasi-one-dimensional electron gas with strong "on-site" interactions, Phys. Rev. B **14**, 2989 (1976).

[7] J. Hubbard, Electron correlations in narrow energy bands, Proc. R. Soc. London A **276**, 238 (1963).

[8] M. C. Gutzwiller, Effect of correlation on the ferromagnetism of transition metals, Phys. Rev. Lett. **10**, 159 (1963).

[9] J. Kanamori, Electron correlation and ferromagnetism of transition metals, Prog. Theor. Phys. **30**, 275 (1963).

[10] J. Hubbard, Electron correlations in narrow energy bands III. An improved solution, Proc. R. Soc. London A **281**, 401 (1964).

[11] R. A. Bari, Effects of short-range interactions on electron-charge ordering and lattice distortions in the localized state, Phys. Rev. B **3**, 2662 (1971).

[12] A. B. Harris and R. V. Lange, Single-particle excitations in narrow energy bands, Phys. Rev. **157**, 295 (1967).

[13] E. Gull, O. Parcollet, P. Werner, and A. J. Millis, Momentum-sector-selective metal-insulator transition in the eight-site dynamical mean-field approximation to the Hubbard model in two dimensions, Phys. Rev. B **80**, 245102 (2009).

[14] W. Wu, M. Ferrero, A. Georges, and E. Kozik, Controlling Feynman diagrammatic expansions: Physical nature of the pseudogap in the two-dimensional Hubbard model, Phys. Rev. B **96**, 041105(R) (2017).

[15] O. Gunnarsson, T. Schäfer, J. P. F. LeBlanc, E. Gull, J. Merino, G. Sangiovanni, G. Rohringer, and A. Toschi, Fluctuation diagnostics of the electron self-energy: Origin of the pseudogap physics, Phys. Rev. Lett. **114**, 236402 (2015).

[16] R. T. Scalettar, E. Y. Loh, J. E. Gubernatis, A. Moreo, S. R. White, D. J. Scalapino, R. L. Sugar, and E. Dagotto, Phase diagram of the two-dimensional negative-U Hubbard model, Phys. Rev. Lett. **62**, 1407 (1989).

[17] H. Shiba, Thermodynamic properties of the one-dimensional half-filled-band Hubbard model. II: Application of the grand canonical method, Prog. Theor. Phys. **48**, 2171 (1972).

[18] C. N. Yang, η pairing and off-diagonal long-range order in a Hubbard model, Phys. Rev. Lett. **63**, 2144 (1989).

[19] S. Zhang, Pseudospin symmetry and new collective modes of the Hubbard model, Phys. Rev. Lett. **65**, 120 (1990).

[20] S. V. Vonsovsky and M. I. Katsnelson, Some types of instabilities in the electron energy spectrum of the polar model of the crystal. I. The maximum-polarity state, J. Phys. C: Solid State Phys. **12**, 2043 (1979).

[21] B. Davoudi and A.-M. S. Tremblay, Non-perturbative treatment of charge and spin fluctuations in the two-dimensional extended Hubbard model: Extended two-particle self-consistent approach, Phys. Rev. B **76**, 085115 (2007).

[22] W. P. Su, Phase separation and d-wave superconductivity in a two-dimensional extended Hubbard model with nearest-neighbor attractive interaction, Phys. Rev. B **69**, 012506 (2004).

[23] M. Yao, D. Wang, and Q.-H. Wang, Determinant quantum Monte Carlo for the half-filled Hubbard model with nonlocal density-density interactions, Phys. Rev. B **106**, 195121 (2022).

[24] W.-C. Chen, Y. Wang, and C.-C. Chen, Superconducting phases of the square-lattice extended Hubbard model, Phys. Rev. B **108**, 064514 (2023).

[25] J. Sólyom, The Fermi gas model of one-dimensional conductors, Adv. Phys. **28**, 201 (1979).

[26] V. J. Emery, Theory of the One-Dimensional Electron Gas, in *Highly Conducting One-Dimensional Solids*, edited by Jozef T. Devreese, Roger P. Evrard, and Victor E. van Doren (Springer US, Boston, 1979), pp. 247–303

[27] B. Fourcade and G. Spronken, Real-space scaling methods applied to the one-dimensional extended Hubbard model. II. The finite-cell scaling method, Phys. Rev. B **29**, 5096 (1984).

[28] Y. Zhang and J. Callaway, Extended Hubbard model in two dimensions, Phys. Rev. B **39**, 9397 (1989).

[29] J. Callaway, D. P. Chen, D. G. Kanhere, and Q. Li, Small-cluster calculations for the simple and extended Hubbard models, Phys. Rev. B **42**, 465 (1990).

[30] X.-Z. Yan, Theory of the extended Hubbard model at half filling, Phys. Rev. B **48**, 7140 (1993).

[31] M. Aichhorn, H. G. Evertz, W. von der Linden, and M. Potthoff, Charge ordering in extended Hubbard models: Variational cluster approach, Phys. Rev. B **70**, 235107 (2004).

[32] B. Davoudi and A.-M. S. Tremblay, Nearest-neighbor repulsion and competing charge and spin order in the extended Hubbard model, Phys. Rev. B **74**, 035113 (2006).

[33] T. Ayral, S. Biermann, and P. Werner, Screening and nonlocal correlations in the extended Hubbard model from

self-consistent combined *GW* and dynamical mean field theory, Phys. Rev. B **87**, 125149 (2013).
[34] H. Hafermann, E. G. C. P. van Loon, M. I. Katsnelson, A. I. Lichtenstein, and O. Parcollet, Collective charge excitations of strongly correlated electrons, vertex corrections, and gauge invariance, Phys. Rev. B **90**, 235105 (2014).
[35] P. Werner and M. Casula, Dynamical screening in correlated electron systems-from lattice models to realistic materials, J. Phys.: Condens. Matter **28**, 383001 (2016).
[36] E. G. C. P. van Loon, M. Schüler, M. I. Katsnelson, and T. O. Wehling, Capturing nonlocal interaction effects in the Hubbard model: Optimal mappings and limits of applicability, Phys. Rev. B **94**, 165141 (2016).
[37] E. A. Stepanov, A. Huber, E. G. C. P. van Loon, A. I. Lichtenstein, and M. I. Katsnelson, From local to nonlocal correlations: The dual boson perspective, Phys. Rev. B **94**, 205110 (2016).
[38] H. Terletska, T. Chen, and E. Gull, Charge ordering and correlation effects in the extended Hubbard model, Phys. Rev. B **95**, 115149 (2017).
[39] G. Rohringer, H. Hafermann, A. Toschi, A. A. Katanin, A. E. Antipov, M. I. Katsnelson, A. I. Lichtenstein, A. N. Rubtsov, and K. Held, Diagrammatic routes to nonlocal correlations beyond dynamical mean field theory, Rev. Mod. Phys. **90**, 025003 (2018).
[40] A. A. Katanin, Extended dynamical mean field theory combined with the two-particle irreducible functional renormalization-group approach as a tool to study strongly correlated systems, Phys. Rev. B **99**, 115112 (2019).
[41] E. A. Stepanov, A. Huber, A. I. Lichtenstein, and M. I. Katsnelson, Effective Ising model for correlated systems with charge ordering, Phys. Rev. B **99**, 115124 (2019).
[42] J. Paki, H. Terletska, S. Iskakov, and E. Gull, Charge order and antiferromagnetism in the extended Hubbard model, Phys. Rev. B **99**, 245146 (2019).
[43] P. Pudleiner, A. Kauch, K. Held, and G. Li, Competition between antiferromagnetic and charge density wave fluctuations in the extended Hubbard model, Phys. Rev. B **100**, 075108 (2019).
[44] E. A. Stepanov, V. Harkov, M. Rösner, A. I. Lichtenstein, M. I. Katsnelson, and A. N. Rudenko, Coexisting charge density wave and ferromagnetic instabilities in monolayer InSe, npj Comput. Mater. **8**, 118 (2022).
[45] M. Vandelli, V. Harkov, E. A. Stepanov, J. Gukelberger, E. Kozik, A. Rubio, and A. I. Lichtenstein, Dual boson diagrammatic Monte Carlo approach applied to the extended Hubbard model, Phys. Rev. B **102**, 195109 (2020).
[46] H. Terletska, S. Iskakov, T. Maier, and E. Gull, Dynamical cluster approximation study of electron localization in the extended Hubbard model, Phys. Rev. B **104**, 085129 (2021).
[47] E. Linnér, A. I. Lichtenstein, S. Biermann, and E. A. Stepanov, Multichannel fluctuating field approach to competing instabilities in interacting electronic systems, Phys. Rev. B **108**, 035143 (2023).
[48] M. Vandelli, A. Galler, A. Rubio, A. I. Lichtenstein, S. Biermann, and E. A. Stepanov, Doping-dependent charge- and spin-density wave orderings in a monolayer of Pb adatoms on Si(111), arXiv:2301.07162.
[49] S. Robaszkiewicz, R. Micnas, and K. A. Chao, Thermodynamic properties of the extended Hubbard model with strong intra-atomic attraction and an arbitrary electron density, Phys. Rev. B **23**, 1447 (1981).
[50] A. Moreo and D. J. Scalapino, Two-dimensional negative-U Hubbard model, Phys. Rev. Lett. **66**, 946 (1991).
[51] M. Randeria, N. Trivedi, A. Moreo, and R. T. Scalettar, Pairing and spin gap in the normal state of short coherence length superconductors, Phys. Rev. Lett. **69**, 2001 (1992).
[52] R. Micnas, J. Ranninger, and S. Robaszkiewicz, Superconductivity in narrow-band systems with local nonretarded attractive interactions, Rev. Mod. Phys. **62**, 113 (1990).
[53] M. Keller, W. Metzner, and U. Schollwöck, Dynamical mean-field theory for pairing and spin gap in the attractive Hubbard model, Phys. Rev. Lett. **86**, 4612 (2001).
[54] M. Capone, C. Castellani, and M. Grilli, First-order pairing transition and single-particle spectral function in the attractive Hubbard model, Phys. Rev. Lett. **88**, 126403 (2002).
[55] A. A. Aligia, Phase diagram of the one-dimensional extended attractive Hubbard model for large nearest-neighbor repulsion, Phys. Rev. B **61**, 7028 (2000).
[56] E. Dagotto, J. Riera, Y. C. Chen, A. Moreo, A. Nazarenko, F. Alcaraz, and F. Ortolani, Superconductivity near phase separation in models of correlated electrons, Phys. Rev. B **49**, 3548 (1994).
[57] A. Toschi, M. Capone, and C. Castellani, Energetic balance of the superconducting transition across the BCS—Bose Einstein crossover in the attractive Hubbard model, Phys. Rev. B **72**, 235118 (2005).
[58] A. Garg, H. R. Krishnamurthy, and M. Randeria, BCS-BEC crossover at $T = 0$: A dynamical mean-field theory approach, Phys. Rev. B **72**, 024517 (2005).
[59] A Toschi, P Barone, M Capone, and C Castellani, Pairing and superconductivity from weak to strong coupling in the attractive Hubbard model, New J. Phys. **7**, 7 (2005).
[60] A. Privitera, M. Capone, and C. Castellani, Finite-density corrections to the unitary Fermi gas: A lattice perspective from dynamical mean-field theory, Phys. Rev. B **81**, 014523 (2010).
[61] A. Koga and P. Werner, Low-temperature properties of the infinite-dimensional attractive Hubbard model, Phys. Rev. A **84**, 023638 (2011).
[62] A. Amaricci, A. Privitera, and M. Capone, Inhomogeneous BCS-BEC crossover for trapped cold atoms in optical lattices, Phys. Rev. A **89**, 053604 (2014).
[63] E. G. C. P. van Loon and M. I. Katsnelson, The extended Hubbard model with attractive interactions, J. Phys.: Conf. Ser. **1136**, 012006 (2018).
[64] A. Tagliavini, M. Capone, and A. Toschi, Detecting a preformed pair phase: Response to a pairing forcing field, Phys. Rev. B **94**, 155114 (2016).
[65] L. Del Re, M. Capone, and A. Toschi, Dynamical vertex approximation for the attractive Hubbard model, Phys. Rev. B **99**, 045137 (2019).
[66] Y.-Y. Xiang, X.-J. Liu, Y.-H. Yuan, J. Cao, and C.-M. Tang, Doping dependence of the phase diagram in one-dimensional extended Hubbard model: A functional renormalization group study, J. Phys.: Condens. Matter **31**, 125601 (2019).
[67] F. C. Zhang, M. Ogata, and T. M. Rice, Attractive interaction and superconductivity for K_3C_{60}, Phys. Rev. Lett. **67**, 3452 (1991).
[68] Y. Wang, Z. Chen, T. Shi, B. Moritz, Z.-X. Shen, and T. P. Devereaux, Phonon-mediated long-range attractive interaction

in one-dimensional cuprates, Phys. Rev. Lett. **127**, 197003 (2021).

[69] V. Meregalli and S. Y. Savrasov, Electron-phonon coupling and properties of doped $BaBiO_3$, Phys. Rev. B **57**, 14453 (1998).

[70] Z. P. Yin, A. Kutepov, and G. Kotliar, Correlation-enhanced electron-phonon coupling: Applications of *GW* and screened hybrid functional to bismuthates, chloronitrides, and other high-T_c superconductors, Phys. Rev. X **3**, 021011 (2013).

[71] M. Tomczyk, S. Lu, J. P. Veazey, M. Huang, P. Irvin, S. Ryu, H. Lee, C.-B. Eom, C. S. Hellberg, and J. Levy, Electron pairing without superconductivity, Nature (London) **521**, 196 (2015).

[72] G. Cheng, M. Tomczyk, A. B. Tacla, H. Lee, S. Lu, J. P. Veazey, M. Huang, P. Irvin, S. Ryu, C.-B. Eom, A. Daley, D. Pekker, and J. Levy, Tunable electron-electron interactions in $LaAlO_3/SrTiO_3$ nanostructures, Phys. Rev. X **6**, 041042 (2016).

[73] M. Tomczyk, G. Cheng, H. Lee, S. Lu, A. Annadi, J. P. Veazey, M. Huang, P. Irvin, S. Ryu, C.-B. Eom, and J. Levy, Micrometer-scale ballistic transport of electron pairs in $LaAlO_3/SrTiO_3$ nanowires, Phys. Rev. Lett. **117**, 096801 (2016).

[74] G. E. D. K. Prawiroatmodjo, M. Leijnse, F. Trier, Y. Chen, D. V. Christensen, M. von Soosten, N. Pryds, and T. S. Jespersen, Transport and excitations in a negative-U quantum dot at the $LaAlO_3/SrTiO_3$ interface, Nat. Commun. **8**, 395 (2017).

[75] D. van der Marel and G. A. Sawatzky, Electron-electron interaction and localization in *d* and *f* transition metals, Phys. Rev. B **37**, 10674 (1988).

[76] H. U. R. Strand, Valence-skipping and negative-U in the d-band from repulsive local Coulomb interaction, Phys. Rev. B **90**, 155108 (2014).

[77] T. Esslinger, Fermi-Hubbard physics with atoms in an optical lattice, Annu. Rev. Condens. Matter Phys. **1**, 129 (2010).

[78] A. N. Rubtsov, Fluctuating local field method probed for a description of small classical correlated lattices, Phys. Rev. E **97**, 052120 (2018).

[79] A. N. Rubtsov, E. A. Stepanov, and A. I. Lichtenstein, Collective magnetic fluctuations in Hubbard plaquettes captured by fluctuating local field method, Phys. Rev. B **102**, 224423 (2020).

[80] Y. S. Lyakhova, E. A. Stepanov, and A. N. Rubtsov, Fluctuating local field approach to free energy of one-dimensional molecules with strong collective electronic fluctuations, Phys. Rev. B **105**, 035118 (2022).

[81] Y. S. Lyakhova and A. N. Rubtsov, Fluctuating local field approach to the description of lattice models in the strong coupling regime, J. Supercond. Nov. Magn. **35**, 2169 (2022).

[82] D. Kuznetsova, G. V. Astretsov, and A. N. Rubtsov, Fluctuating local field method for the disordered Ising model, arXiv:2212.14733 (2022).

[83] See Supplemental Material at http://link.aps.org/supplemental/10.1103/PhysRevB.108.205156 for a detailed description of the MCFF approach applied to the extended Hubbard model, including a definition of the calculated quantities and a derivation of the variational construction of MCFF trial action.

[84] R. Peierls, On a minimum property of the free energy, Phys. Rev. **54**, 918 (1938).

[85] N. N. Bogolyubov, A variation principle in the problem of many bodies, Dokl. Akad. Nauk SSSR (Russian Academy of Sciences) **119**, 244 (1958).

[86] R. P. Feynman, *Statistical Mechanics: A Set of Lectures* (Benjamin/Cummings, Reading, 1972).

[87] F. Šimkovic, J. P. F. LeBlanc, A. J. Kim, Y. Deng, N. V. Prokof'ev, B. V. Svistunov, and E. Kozik, Extended crossover from a Fermi liquid to a quasiantiferromagnet in the half-filled 2D Hubbard model, Phys. Rev. Lett. **124**, 017003 (2020).

[88] A. P. Itin and A. I. Neishtadt, Effective Hamiltonians for fastly driven tight-binding chains, Phys. Lett. A **378**, 822 (2014).

[89] A. P. Itin and M. I. Katsnelson, Effective Hamiltonians for rapidly driven many-body lattice systems: Induced exchange interactions and density-dependent hoppings, Phys. Rev. Lett. **115**, 075301 (2015).

[90] M. Bukov, M. Kolodrubetz, and A. Polkovnikov, Schrieffer-Wolff transformation for periodically driven systems: Strongly correlated systems with artificial gauge fields, Phys. Rev. Lett. **116**, 125301 (2016).

[91] C. Dutreix and M. I. Katsnelson, Dynamical control of electron-phonon interactions with high-frequency light, Phys. Rev. B **95**, 024306 (2017).

[92] C. Dutreix, E. A. Stepanov, and M. I. Katsnelson, Laser-induced topological transitions in phosphorene with inversion symmetry, Phys. Rev. B **93**, 241404(R) (2016).

[93] E. A. Stepanov, C. Dutreix, and M. I. Katsnelson, Dynamical and reversible control of topological spin textures, Phys. Rev. Lett. **118**, 157201 (2017).

[94] V. N. Valmispild, C. Dutreix, M. Eckstein, M. I. Katsnelson, A. I. Lichtenstein, and E. A. Stepanov, Dynamically induced doublon repulsion in the Fermi-Hubbard model probed by a single-particle density of states, Phys. Rev. B **102**, 220301(R) (2020).

[95] M. A. Sentef, Light-enhanced electron-phonon coupling from nonlinear electron-phonon coupling, Phys. Rev. B **95**, 205111 (2017).

[96] E. Berger, P. Valášek, and W. von der Linden, Two-dimensional Hubbard-Holstein model, Phys. Rev. B **52**, 4806 (1995).

[97] G. Sangiovanni, M. Capone, C. Castellani, and M. Grilli, Electron-phonon interaction close to a Mott transition, Phys. Rev. Lett. **94**, 026401 (2005).

[98] P. Werner and A. J. Millis, Efficient Dynamical mean field simulation of the Holstein-Hubbard model, Phys. Rev. Lett. **99**, 146404 (2007).

[99] J. G. Bednorz and K. A. Müller, Possible high T_c superconductivity in the Ba-La-Cu-O system, Z. Phys. B **64**, 189 (1986).

[100] J. D. Jorgensen, B. Dabrowski, Shiyou Pei, D. G. Hinks, L. Soderholm, B. Morosin, J. E. Schirber, E. L. Venturini, and D. S. Ginley, Superconducting phase of $La_2CuO_{4+\delta}$: A superconducting composition resulting from phase separation, Phys. Rev. B **38**, 11337 (1988).

[101] K. Machida, Magnetism in La_2CuO_4 based compounds, Phys. C **158**, 192 (1989).

[102] J. Zaanen and O. Gunnarsson, Charged magnetic domain lines and the magnetism of high-T_c oxides, Phys. Rev. B **40**, 7391 (1989).

[103] M. Kato, K. Machida, H. Nakanishi, and M. Fujita, Soliton lattice modulation of incommensurate spin density wave in two dimensional Hubbard model—A mean field study, J. Phys. Soc. Jpn. **59**, 1047 (1990).

[104] V. J. Emery and S. A. Kivelson, Frustrated electronic phase separation and high-temperature superconductors, Phys. C **209**, 597 (1993).

[105] B. W. Statt, P. C. Hammel, Z. Fisk, S-W. Cheong, F. C. Chou, D. C. Johnston, and J. E. Schirber, Oxygen ordering and phase separation in $La_2CuO_{4+\delta}$, Phys. Rev. B **52**, 15575 (1995).

[106] M. Fratini, N. Poccia, A. Ricci, G. Campi, M. Burghammer, G. Aeppli, and A. Bianconi, Scale-free structural organization of oxygen interstitials in La_2CuO_{4+y}, Nature (London) **466**, 841 (2010).

[107] N. Poccia, A. Ricci, G. Campi, M. Fratini, A. Puri, D.D. Gioacchino, A. Marcelli, M. Reynolds, M. Burghammer, N.L. Saini, and G. Aeppli, Optimum inhomogeneity of local lattice distortions in La_2CuO_{4+y}, Proc. Natl. Acad. Sci. USA **109**, 15685 (2012).

[108] G. Campi, A. Bianconi, N. Poccia, G. Bianconi, L. Barba, G. Arrighetti, D. Innocenti, J. Karpinski, N. D. Zhigadlo, S. M. Kazakov, M. Burghammer, M. v. Zimmermann, M. Sprung, and A. Ricci, Inhomogeneity of charge-density-wave order and quenched disorder in a high-T_c superconductor, Nature (London) **525**, 359 (2015).

[109] J. Wu, O. Pelleg, G. Logvenov, A. T. Bollinger, Y-J. Sun, G. S. Boebinger, M. Vanević, Z. Radović, and I. Božović, Anomalous independence of interface superconductivity from carrier density, Nat. Mater. **12**, 877 (2013).

[110] T. Misawa, Y. Nomura, S. Biermann, and M. Imada, Self-optimized superconductivity attainable by interlayer phase separation at cuprate interfaces, Sci. Adv. **2**, e1600664 (2016).

[111] Y. Kamihara, H. Hiramatsu, M. Hirano, R. Kawamura, H. Yanagi, T. Kamiya, and H. Hosono, Iron-based layered superconductor: LaOFeP, J. Am. Chem. Soc. **128**, 10012 (2006).

[112] H. Takahashi, K. Igawa, K. Arii, Y. Kamihara, M. Hirano, and H. Hosono, Superconductivity at 43 K in an iron-based layered compound $LaO_{1-x}F_xFeAs$, Nature (London) **453**, 376 (2008).

[113] A. Ricci, N. Poccia, G. Campi, B. Joseph, G. Arrighetti, L. Barba, M. Reynolds, M. Burghammer, H. Takeya, Y. Mizuguchi, Y. Takano, M. Colapietro, N. L. Saini, and A. Bianconi, Nanoscale phase separation in the iron chalcogenide superconductor $K_{0.8}Fe_{1.6}Se_2$ as seen via scanning nanofocused x-ray diffraction, Phys. Rev. B **84**, 060511(R) (2011).

[114] M. Bendele, A. Barinov, B. Joseph, D. Innocenti, A. Iadecola, A. Bianconi, H. Takeya, Y. Mizuguchi, Y. Takano, T. Noji, T. Hatakeda, Y. Koike, M. Horio, A. Fujimori, D. Ootsuki, T. Mizokawa, and N. L. Saini, Spectromicroscopy of electronic phase separation in $K_xFe_{2-y}Se_2$ superconductor, Sci. Rep. **4**, 5592 (2014).

[115] L. Simonelli, T. Mizokawa, M. M. Sala, H. Takeya, Y. Mizuguchi, Y. Takano, G. Garbarino, G. Monaco, and N. L. Saini, Temperature dependence of iron local magnetic moment in phase-separated superconducting chalcogenide, Phys. Rev. B **90**, 214516 (2014).

[116] A. Ricci, N. Poccia, B. Joseph, D. Innocenti, G. Campi, A. Zozulya, F. Westermeier, A. Schavkan, F. Coneri, A. Bianconi, H. Takeya, Y. Mizuguchi, Y. Takano, T. Mizokawa, M. Sprung, and N. L. Saini, Direct observation of nanoscale interface phase in the superconducting chalcogenide $K_xFe_{2-y}Se_2$ with intrinsic phase separation, Phys. Rev. B **91**, 020503(R) (2015).